

# Performance Analysis of TeraHertz Unmanned Aerial Vehicular Networks

Xufang Wang, *Member, IEEE*, Peng Wang, *Member*, Ming Ding, *Senior member*, Zihuai Lin, *Senior member*, Feng Lin, Branka Vucetic, *Fellow* and Lajos Hanzo, *Fellow*

**Abstract**—*TeraHertz* (THz) transmission technologies constitute a promising candidate for supporting ultra-broadband short-range next generation communications. Hence, we analyse the performance of *unmanned aerial vehicle* (UAV) in the THz networks. The coverage probability is derived as well as the *area spectral efficiency* (ASE) and a pair of *Line-of-sight* (LoS)/*non-line-of-sight* (NLoS) probability models, namely the *macrocell LoS/NLoS* probability model and *picocell LoS/NLoS* probability model are adopted. Furthermore, the lower-bound of the network performance are derived via *homogeneous Poisson point process* (HPPP) analysis, as well as the upper-bound. The simulation results match the analytical results well, which show that the coverage probability of the network first increases upon increasing the THz UAV BS density, and then decreases beyond the maximum. Given the severe path loss experienced by THz signals, a higher UAV density is required for a certain coverage probability than at lower carrier frequencies.

**Index Terms**—THz, UAV, stochastic geometry, coverage probability, area spectral efficiency

## I. INTRODUCTION

In the past few decades, wireless communication has experienced an explosive growth owing to our request for high speed data connection anywhere and anytime. Thus, wireless *Terabit-per-second* (Tbps) links are sought right across the globe [1]. However, it is not feasible to achieve Tbps data rates with low carrier frequencies which exhibit benign propagation properties, not even at *millimeter wave* (mm-Wave) 60 *Giga-Hertz* (GHz) carrier frequencies, due to the limited bandwidth. The *TeraHertz* (THz)-band (0.1-10 THz) [2], therefore, is regarded as a key technology capable of providing unprecedented data rates for *next generation networks* (NGN). Indeed,

Copyright (c) 2020 IEEE. Personal use of this material is permitted. However, permission to use this material for any other purposes must be obtained from the IEEE by sending a request to pubs-permissions@ieee.org.

This work is funded by Fujian Provincial Department of Science and Technology Project Grant (2019J01267). The work of Z. Lin is supported in part by the Australian Research Council (ARC) Discovery Project DP190101988. The work of B. Vucetic is supported in part by the ARC Laureate Fellowship grant number FL160100032. L. Hanzo would like to acknowledge the financial support of the Engineering and Physical Sciences Research Council projects EP/N004558/1, EP/P034284/1, EP/P034284/1, EP/P003990/1 (COALESCE), of the Royal Society's Global Challenges Research Fund Grant as well as of the European Research Council's Advanced Fellow Grant QuantCom. (*Corresponding author: Lajos Hanzo.*)

Xufang Wang is with Key Laboratory of OptoElectronic Science and Technology for Medicine of Ministry of Education, Fujian Provincial Key Laboratory of Photonics Technology, Fujian Normal University, Fuzhou, China, e-mail: fzwxf@qq.com.

Peng Wang, Zihuai Lin and Branka Vucetic are with the School of Electrical and Information Engineering, University of Sydney, Sydney, Australia, e-mail: {thomaspeng.wang, zihuai.lin,branka.vucetic}@sydney.edu.au

Ming Ding is with Data61, CSIRO, Eveleigh, NSW 2015, Australia, e-mail: Ming.Ding@data61.csiro.au

Feng Lin is with Fuzhou Institute for Data Technology, Fuzhou, China, e-mail: helloyou@189.cn

Lajos Hanzo is with University of Southampton, UK, e-mail: lh@ecs.soton.ac.uk

THz band communications has been made more feasible by the cutting-edge research on propagation [3], [4] and channel modeling [1], just to name a few of the radical advances.

Besides the high path-loss at this high frequency, absorption by water vapor molecules becomes the main factor affecting the propagation of THz-band signals [5]. Moreover, since the surfaces regarded as being smooth at high wavelength in the conventional frequency band become classified as rough in the THz band, the interference imposed by NLoS propagation should also be considered [6]. The THz *base station* (BS) densities can be very high due to the high path loss and absorption without imposing excessive inter-cell-interference. For traditional systems, a general path loss model is assumed for deriving the analytical results of coverage probability [7], which is not applicable to THz networks. In order to analytically characterize a THz network, we use a stochastic geometry tool in this paper, which has been widely employed in the modeling and analysis of conventional low-carrier communication networks, especially for interference and coverage analysis. However, there is a paucity of studies on the interference and coverage probability of THz band communications relying on stochastic geometry. To appraise the literature, the performance analysis on the mean interference power and outage probability for 0.1–10 THz is provided in [8]. The mean interference analysis was then extended to band-limited Terahertz band communications in [9]. The *signal-to-interference-noise-ratio* (SINR) and the coverage probabilities of THz band communication at a certain frequency were calculated for beamforming aided AP in [6]. The stochastic interference modeling of pulse-based TeraHertz communication was investigated in [2].

Some of the challenges of high-speed UAV communications can be mitigated by relying on the THz-band. More explicitly, UAVs can provide broadband communications by moving across a large-scale area [10], [11], for example, for supporting emergency services and surveillance across disaster-affected regions via forming *flying ad hoc networks* (FANETs) [12]. UAVs have already been used for THz spectroscopy to detect atmospheric molecules [13] and they can also be harnessed for THz communications. Although THz signals suffer from a high pathloss, compared to THz base stations on the ground, the probability of benign propagation from the Unmanned Aerial Vehicular (UAV) THz base stations to the users is typically high, since the UAVs are capable of adjusting their coverage area based on the users that they have to serve and on the surrounding environment. Hence, they are capable of reducing the pathloss. In [14], the feasibility of employing the THz-band (0.75–10 THz) for communications at different altitudes among UAVs has been evaluated. Moreover, high-speed communication links can also be established within the

THz band between dynamically roaming objects, rendering THz a realistic candidate for UAV application scenarios [15]. Meanwhile, THz hardware research is also developing rapidly. The transmitter and receiver can be implemented relying on Graphene technology [1] and THz antennas can be quite compact [15]. Hence they can be mounted on UAVs. However, the performance of THz UAV networks has not been investigated in the literature before.

Hence we present the performance analysis of a UAV-enabled THz network in this paper. Both the coverage probability and the ASE are derived and a pair of LOS/NLOS probability models, namely a macrocell LoS/NLoS probability model and a picocell LoS/NLoS probability model are considered. In addition, not only the lower-bound of the THz UAV network performance is obtained but also the upper-bound. We also included Table I for boldly and demonstratively the novelty of our paper.

This paper is organized as follows. In Section II we introduce the system model of THz UAV networks and the LOS/NLOS probability models. The analytical expressions of the coverage probability and the ASE of the THz UAV network are derived by relying on *Poisson point process* (PPP)-distribution in Section III. Simulation and discussions are provided in Section IV. Finally, Section V concludes this paper.

## II. SYSTEM MODEL

Let us now consider a THz UAV network, in which the THz UAV aerial BSs obey a 2D-PPP distribution on an elevated plane with the BS density denoted by  $\rho$  in an infinite 2D space  $\Theta$ . We set the UAV height as a variable  $H$ . Thus, we have  $\Theta = \{(x, y) : x, y \in R\}$  and the coordinates of the UAV are  $(x, y, H)$ .  $H$  is less than 100 m in order to avoid the network capacity reduction observed in [7]. *User equipment* (UEs) are Poisson distributed in the network under consideration and its density is represented by  $\rho_{UE}$ , assuming that the density is higher than  $\rho$  to ensure that each UAV within its coverage has at least one associated UE. The system model of the THz UAV network is depicted in Fig. 1.

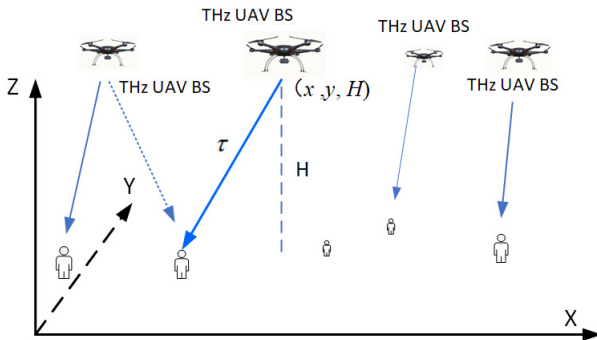


Fig. 1. The system model of the THz UAV network.

The distance between an arbitrary UE and an arbitrary THz UAV BS is denoted by  $\tau$  in km, so we have  $\tau = \sqrt{x^2 + y^2 + H^2}$ . Since the THz channel is highly frequency-selective together with the non-white molecular absorption

noise, the path loss function of THz UAV networks is strongly related to the frequency. The path loss function of THz UAV networks associated with the distance  $\tau$  and the frequency  $f$  is denoted by  $\xi(\tau, f)$ . Both LoS and NLoS transmissions are considered here. Let  $\xi^L(\tau, f)$  and  $\xi^{NL}(\tau, f)$  denote the path loss functions of LoS and NLoS, respectively, then we have [7]

$$\xi(\tau, f) = \begin{cases} \xi^L(\tau, f), & \text{with probability } P^L(\tau), \\ \xi^{NL}(\tau, f), & \text{with probability } 1 - P^L(\tau), \end{cases} \quad (1)$$

together with the LoS probability function  $P^L(\tau)$ . The path loss of the THz LOS channel is given by [9]

$$\xi^L(\tau, f) = \frac{c^2}{(4\pi\tau f)^2} \exp[-\varepsilon(f)\tau], \quad (2)$$

where  $\varepsilon(f)$  is the absorption coefficient at frequency  $f$ , and  $c$  is the speed of light. By contrast, the path loss of the THz NLOS channel is given by [16]

$$\xi^{NL}(\tau, f) = \frac{c^2\beta(f)}{(4\pi\tau f)^2} \exp[-\varepsilon(f)\tau], \quad (3)$$

where  $\beta(f)$  is the scattering loss coefficient of the NLOS path at frequency  $f$ .

Since there is no consensus in the literature on the most accurate LoS/NLoS probability model for UAV-enabled networks, a pair of widely adopted LoS/NLoS probability models [12] are considered here for the THz UAV networks.

### A. Macrocell LoS/NLoS probability model

For the macrocell THz UAV BSs, we adopt the 3GPP macrocell-to-UE model [17] as the LoS/NLoS probability model with the LoS probability function expressed by

$$P_{macro}^L(\tau) = [1 - \exp(-\tau/0.063)] \cdot \min(0.018/\tau, 1) + \exp(-\tau/0.063). \quad (4)$$

### B. Picocell LoS/NLoS probability model

For the picocell THz BSs, the 3GPP picocell-to-UE model [17] is introduced as the LoS/NLoS probability model with the LoS probability function given by

$$P_{pico}^L(\tau) = \min[0.5, 5 \exp(-\tau/0.03)] + 0.5 - \min[0.5, 5 \exp(-0.156/\tau)]. \quad (5)$$

## III. PERFORMANCE ANALYSIS FOR THz UAV NETWORKS

In this section, not only is the coverage probability of the THz UAV network theoretically derived based on the LOS and NLOS THz path loss models, but also the ASE. The THz channel is highly frequency-selective and several transmission windows are formed by the THz path loss peak due to molecular absorption[16]. In addition, noise reduction factor caused by quantum effects also has impact on high frequencies [9]. Therefore, we can adaptively divide the total bandwidth into numerous sub-bands, say  $m$  sub-bands. The  $i$ -th sub-band is centered around frequency  $f_i, i = 1, 2, \dots, m$  and

TABLE I

	our paper	[16]-2014	[7]-2016	[4]-2017	[6]-2017	[8]-2017	[10]-2018	[11]-2018	[12]-2018	[2]-2019	[3]-2020
THz Communications	✓	✓		✓	✓	✓				✓	✓
UAV	✓						✓	✓	✓		
Stochastic Geometry Analysis	✓		✓		✓	✓			✓		
Coverage Probability	✓		✓		✓				✓		
Area Spectral Efficiency (ASE)	✓		✓						✓		
LOS and NLOS probability models	✓		✓						✓		

it has a width of  $w_{f_i}$ . If  $w_{f_i}$  is small enough, the channel can be regarded as frequency-non-selective and the noise power spectral density appears to be locally flat.

The SINR of the subband at frequency  $f_i$  can be expressed as:

$$\Gamma(f_i) = \frac{V_i g \xi(\tau, f_i)}{I_\tau(f_i) + N(f_i)}, \quad (6)$$

where  $V_i$  denotes the transmission power of the  $i$ th THz subband at the THz UAV-BS;  $g$  is the Rayleigh fading channel gain [18] modeled as an exponential *random variable* (RV) with the mean of one;  $N_o(f_i)$  denotes the noise power at frequency  $f_i$  for each UE;  $I_\tau(f_i)$  is the cumulative interference arriving from all the other THz UAV-BSs at frequency  $f_i$  given by

$$I_\tau(f_i) = \sum_{j: b_j \in \psi / b_s} V_j \xi_j(f_i) g_j, \quad (7)$$

where  $b_s$  is the serving THz UAV BS positioned at distance  $\tau$  from UE, and  $b_j$  in (7) is the  $j$ th interfering THz UAV BS, while the path loss at frequency  $f_i$  and the multipath fading channel gain of which are denoted by  $\xi_j(f_i)$  and  $g_j$ , respectively;  $\psi$  denotes the set of active THz UAV BS as idle BSs do not generate interference. The noise power  $N_o(f_i)$  in (6) is given by

$$N_o(f_i) = k_b T N_f n_f(f_i), \quad (8)$$

where  $k_b$  is the Boltzmann constant;  $T$  is the temperature;  $N_f$  is the noise figure;  $n_f(f_i)$  is a noise reduction factor at frequency  $f_i$  caused by quantum effects at high frequencies [9], which is expressed as

$$n_f(f_i) = \frac{h f_i}{k_b T} \left[ \exp\left(\frac{h f_i}{k_b T}\right) - 1 \right]^{-1}, \quad (9)$$

where  $h$  is Planck's constant.

Naturally, we will avoid using the THz spectral regions having strong absorption and noise. Let  $Z$  denote the transmission power of the THz UAV BS. The power of the  $i$ -th sub-band is denoted by  $V_i$  which satisfies

$$\sum_i V_i = Z. \quad (10)$$

The channel capacity  $C(\tau)$  is expressed by

$$C(\tau) = \sum_i w_{f_i} \log_2 \left[ 1 + \frac{V_i g \xi(\tau, f_i)}{N(f_i)} \right], \quad (11)$$

where  $V_i$  is chosen to satisfy the equal power allocation condition as follows:

$$V_i = \frac{Z}{m}. \quad (12)$$

The coverage probability is defined as the probability that the received SINR is higher than a pre-set threshold  $\eta$ . Thus, we can express the coverage probability for the subband at frequency  $f_i$  of the THz UAV network as:

$$P_c(\rho, \eta, f_i) = \Pr(\Gamma(f_i) > \eta), \quad (13)$$

When the geographic distribution of the THz UAV-BSs obeys a HPPP and they are randomly positioned in the network, the THz UAV network performance gets its lower bound [12]. This lower-bound performance is formulated by Theorem 1.

**Theorem 1.** *The lower-bound of the coverage probability of a THz UAV network at frequency  $f_i$  can be formulated as*

$$P_{c,low}(\rho, \eta, f_i) = \int_H^\infty \Lambda^L \varphi^L(\tau) d\tau + \int_H^\infty \Lambda^{NL} \varphi^{NL}(\tau) d\tau \quad (14)$$

where  $\Lambda^L = \Pr\left[\frac{V_i g \xi^L(\tau, f_i)}{I_\tau(f_i) + N(f_i)} > \eta\right]$ ,  $\Lambda^{NL} = \Pr\left[\frac{V_i g \xi^{NL}(\tau, f_i)}{I_\tau(f_i) + N(f_i)} > \eta\right]$ ;  $\varphi^L(\tau)$  and  $\varphi^{NL}(\tau)$  are given by

$$\begin{aligned} \varphi^L(\tau) &= 2\pi\tau\rho P^L(\tau) \cdot \exp\left\{-2\pi\rho \int_H^{\tau_a} [1 - P^L(v)] v dv\right\} \\ &\cdot \exp\left\{2\pi\rho \int_H^\tau P^L(v) v dv\right\}, \end{aligned} \quad (15)$$

$$\begin{aligned} \varphi^{NL}(\tau) &= 2\pi\tau\rho [1 - P^L(\tau)] \exp\left[-2\pi\rho \int_H^{\tau_b} P^L(v) v dv\right] \\ &\cdot \exp\left(-2\pi\rho \int_H^\tau [1 - P^L(v)] v dv\right), \end{aligned} \quad (16)$$

where

$$\tau_a = \arg[\xi^{NL}(\tau_a, f_i) = \xi^L(\tau, f_i)] \quad (17)$$

and

$$\tau_b = \arg[\xi^L(\tau_b, f_i) = \xi^{NL}(\tau, f_i)], \quad (18)$$

respectively. Furthermore, we have

$$A^L = \exp \left[ -\frac{\eta N(f_i)}{V_i \xi^L(\tau, f_i)} \right] \cdot \mathcal{S}_1 \quad (19)$$

and

$$A^{NL} = \exp \left[ -\frac{\eta N(f_i)}{V_i \xi^{NL}(\tau, f_i)} \right] \cdot \mathcal{S}_2, \quad (20)$$

where

$$\begin{aligned} \mathcal{S}_1 &= \mathcal{L}_{I_\tau}^L \left[ \frac{\eta}{V_i \xi^L(\tau, f_i)} \right] \\ &= \exp \left[ -2\pi\rho \int_\tau^{+\infty} \frac{P^L(v)}{1 + \eta^{-1}} v dv \right] \\ &\cdot \exp \left[ -2\pi\rho \int_{\tau_a}^{+\infty} \frac{1 - P^L(v)}{1 + (\alpha\eta)^{-1}} v dv \right] \end{aligned} \quad (21)$$

and

$$\begin{aligned} \mathcal{S}_2 &= \mathcal{L}_{I_\tau}^{NL} \left[ \frac{\eta}{V_i \xi^{NL}(\tau, f_i)} \right] \\ &= \exp \left[ -2\pi\rho \int_{\tau_b}^{+\infty} \frac{P^L(v)}{1 + \left(\frac{\eta}{\alpha}\right)^{-1}} v dv \right] \\ &\cdot \exp \left[ -2\pi\rho \int_\tau^{+\infty} \frac{1 - P^L(v)}{1 + \eta^{-1}} v dv \right], \end{aligned} \quad (22)$$

where  $\mathcal{L}_{I_\tau}$  is the Laplace transform of  $I_\tau(f_i)$  in the computation of interference and

$$\alpha = \beta(f_i). \quad (23)$$

*Proof:* See Appendix A. ■

The computation results of  $\tau_a$  and  $\tau_b$  can be expressed by

$$\tau_a = \frac{2}{\varepsilon(f_i)} \text{LambertW}_0 \left( \frac{\varepsilon(f_i)\tau}{2} \sqrt{\beta(f_i) e^{\tau\varepsilon(f_i)}} \right) \quad (24)$$

and

$$\tau_b = \frac{2}{\varepsilon(f_i)} \text{LambertW}_0 \left( \frac{\varepsilon(f_i)\tau}{2} \sqrt{\frac{e^{\tau\varepsilon(f_i)}}{\beta(f_i)}} \right). \quad (25)$$

On the other hand, as the LOS probability functions according to our two models (4) and (5) are monotone decreasing, the LOS probability is maximized from the overhead hovering UAV with the distance  $\tau = H$ . Thus the received signal power of the user is also maximized in this case. Therefore, the THz UAV network performance can reach the upper-bound when each THz UAV BS is right over the associated user's head [12], which can be derived from Theorem 1 and described by Lemma 2.

**Lemma 2.** *The upper-bound of the coverage probability of a THz UAV network at frequency  $f_i$  can be expressed as*

$$\begin{aligned} &P_{c, \text{upper}}(\rho, \eta, f_i) \\ &= \Pr \left[ \frac{V_i g \xi^{NL}(H, f_i)}{I_\tau(f_i) + N(f_i)} > \eta \right] + \Pr \left[ \frac{V_i g \xi^L(H, f_i)}{I_\tau(f_i) + N(f_i)} > \eta \right] \\ &= \mathcal{L}_{I_\tau}^L \left[ \frac{\eta}{V_i \xi^L(H, f_i)} \right] \cdot \exp \left( -\frac{\eta N(f_i)}{V_i \xi^L(H, f_i)} \right) \\ &\quad + \mathcal{L}_{I_\tau}^{NL} \left[ \frac{\eta}{V_i \xi^{NL}(H, f_i)} \right] \cdot \exp \left( -\frac{\eta N(f_i)}{V_i \xi^{NL}(H, f_i)} \right). \end{aligned} \quad (26)$$

As seen from Theorem 1 and Lemma 2, the lower-bound and upper-bound of the coverage probability of a THz UAV network can be expressed in the form of two terms, corresponding to the LOS and NLOS transmission, respectively.

Additionally, we also analyze another performance metric, namely the *area spectral efficiency* (ASE) [7] of a THz UAV network. ASE quantifies the spectral efficiency of cellular systems in bps/Hz/km<sup>2</sup> with the spatial characteristics taken into account. In prose, this is defined as the sum of the maximum average data rates per unit bandwidth per unit area supported by a base station. According to [7], the ASE of the THz UAV network for a subband at the center frequency of  $f_i$  can be formulated as:

$$\Psi(\rho, \eta, f_i) = \rho \int_\eta^\infty \log_2(1+u) \sigma(\rho, u, f_i) du. \quad (27)$$

Based on the definition of  $P_c(\rho, \eta, f_i)$  in (13), which is the *complementary cumulative distribution function* (CCDF) of the SINR, the *probability density function* (PDF) of the SINR  $\eta$  observed at the typical UE for a particular value  $\rho$ , i.e.,  $\sigma(\rho, \eta, f_i)$  can be expressed as:

$$\sigma(\rho, \eta, f_i) = \frac{\partial [1 - P_c(\rho, \eta, f_i)]}{\partial \eta}. \quad (28)$$

According to the partial integration theorem, we have

$$\begin{aligned} \Psi(\rho, \eta, f_i) &= \rho \log_2(1+\eta) P_c(\rho, \eta, f_i) \\ &\quad + \frac{\rho}{\ln 2} \int_\eta^{+\infty} \frac{P_c(\rho, u, f_i)}{1+u} du. \end{aligned} \quad (29)$$

Thus, by substituting  $P_c(\rho, \eta, f_i)$  in (14) and (26) into (29), the corresponding ASE of THz UAV networks can be obtained.

#### IV. SIMULATION RESULTS AND DISCUSSION

Simulations have been carried out in this section to demonstrate not only the coverage probability but also the ASE of THz networks by two UAV LoS probability models. First, we simulate THz UAVs at the height of 30 m, applying the macrocell LoS/NLoS probability model of (4). There is a THz transmission window at 350 GHz [16]. Thus, the simulation parameters are shown in Table II<sup>1</sup>. The simulations are conducted in Matlab and 100,000 random runs are performed.

TABLE II  
SIMULATION PARAMETERS

Parameters	Symbols	Values
Center frequency of the subband	$f_1$	350 GHz
Power of the subband	$V_1$	-48 dBm/Hz
SNR threshold for the subband	$\gamma_1$	0.1
Noise power	$N(f_1)$	-174 dBm (according to (8))

<sup>1</sup>The bandwidth of the THz signals has not been determined explicitly in the paper. We are interested in the property of a particular subband at a certain frequency since the THz band is highly frequency-selective. If the bandwidth is 2GHz, the total power of terahertz signals would be about 32 W, which is reasonable for an outdoor THz Base Station.

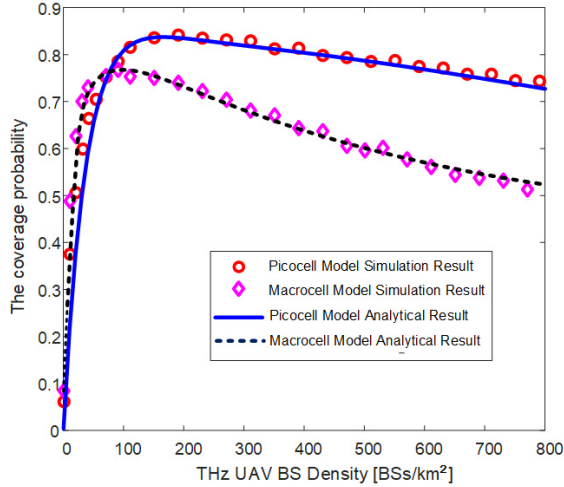


Fig. 2. The coverage probabilities calculated from Eq. (14) and simulated for hovering THz UAVs at  $h=30$  m (by macrocell LoS/NLoS probability model) and  $h=10$  m (by picocell LoS/NLoS probability model).

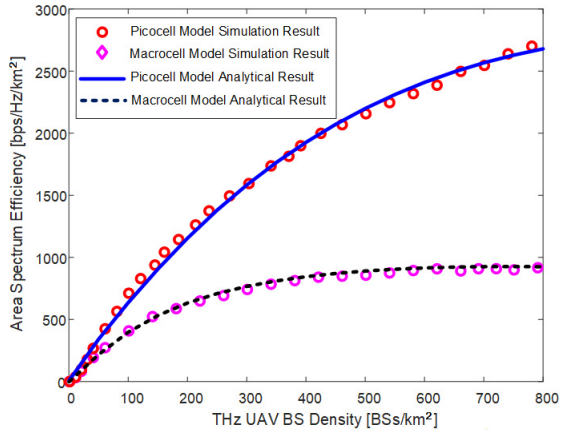


Fig. 3. The ASE calculated from Eq. (29) and simulated for hovering THz UAVs at  $h=30$  m (by macrocell LoS/NLoS probability model) and  $h=10$  m (by picocell LoS/NLoS probability model).

The coverage probability and the ASE achieved by hovering THz UAVs ( $h=30$ m) relying on the macrocell<sup>2</sup> LoS/NLoS probability model are shown in Fig. 2 and Fig. 3, respectively. It can be seen that the coverage probability increases rapidly to near 0.9 and then gradually decreases, which can be explained as follows: when the THz UAV BSs density is too low, the received signal quality of the typical UE becomes better as the UAV density increases and the probability of LOS transmission from the UAV gets higher, hence the coverage probability increases rapidly. However, when the BS density reaches a certain level, the co-channel interference from other UAVs also becomes stronger, which overwhelms the desired received signal of UE, so the coverage probability begins to decay after reaching the optimal point. The UAV density of the highest coverage probability is about 200 BSs per  $\text{km}^2$ , which

<sup>2</sup>Based on the UAV altitude being 30 and 10 m, the scenarios is reminiscent of the terrestrial macro and pico-cell antenna heights. Hence we refer to them as macro- and pico-cells, noting that the associated coverage areas are smaller than those of the typical macro-and pic-cells.

is much denser than the BS density at microwave frequencies [12]. This is because the THz signal experiences much higher path loss than the conventional microwave frequencies. In order to keep the coverage probability comparable to conventional radio frequency signals, high beam forming gains are required for THz UAV networks. The optimal THz UAV density can also be obtained by setting the partial derivative of the coverage probability with respect to  $\rho$  to zero, i.e.,  $\rho_0 = \arg \left\{ \frac{P_c(\rho, \eta, f_i)}{\rho} = 0 \right\}$ , which is closely related to the parameters, such as  $f_i$ ,  $\eta$ , etc.

Observe from Fig. 3 that the ASE grows rapidly upon increasing the BS densities, but the gradient becomes lower as the density of UAVs becomes higher than about 200 BSs/ $\text{km}^2$ , which is the UAV density, when the coverage probability reaches its maximum in Fig. 2. Given the severe path loss of THz interference, the ASE does not drop so dramatically upon increasing the UAV density as in the conventional microwave radio frequency signals [7]. It can also be observed from Fig.2 and Fig. 3 that our analytical results match the simulation results very well, which is quite reassuring.

Then we also simulated THz UAVs at the height of 10 m, i.e.,  $h=10$  m, applying the picocell LoS/NLoS probability model of Eq. (5). The simulation parameters are the same as those used for the macrocell LoS/NLoS probability model. The coverage probability and the ASE for hovering THz UAVs ( $h=10$  m) obeying the picocell LoS/NLoS probability model are also shown in Fig. 2 and Fig. 3, respectively. Observed that the coverage probability rapidly first increases and then decreases after reaching its maximum around 100 UAV BSs per  $\text{km}^2$ . The maximum coverage probability of the picocell probability model THz UAV network is higher than that of the macrocell probability model at the same THz UAV BS density. This is due to the more severe path loss of the macrocell THz UAV BSs. The ASE of the picocell probability model THz UAV network is also higher than that of the macrocell probability model at the same UAV density. It can also be seen from Fig.2 and Fig. 3 that our analytical results match well the simulation results.

## V. CONCLUSIONS

The performance of a UAV-aided THz network was analyzed theoretically in this paper. The analytical coverage probability and ASE expressions were derived. Furthermore, we obtain the lower-bound and upper-bound of the THz network performance. Our results demonstrated that the coverage probability of the network first increases with the density of THz UAV BSs, and then decreases beyond the maximum value. Considering the severe path loss suffered by THz signals, a higher UAV density is required for a certain coverage probability compared to lower carrier frequencies. As our future work, in our analysis we will consider introducing Rician fading or Nakagami fading for the LoS transmissions as the multi-path fading model. Moreover, the *delay-sensitive area spectral efficiency* (DASE) [19] of THz UAV networks will also be considered in our future research.

APPENDIX A  
PROOF OF THEOREM 1

*Proof:* According to [7] we calculate  $\Pr(\Gamma(f_i) > \eta)$  for the LoS and the NLoS cases conditioned on  $\tau$ . From (13) and (6), we can show that

$$\begin{aligned}
 P_{c, \text{low}}(\rho, \eta, f_i) &= \int_H^\infty \Pr(\Gamma(f_i) > \eta | \tau) \varphi(\tau) d\tau \\
 &= \int_H^\infty \Pr\left(\frac{V_i g \xi(\tau, f_i)}{I_\tau(f_i) + N(f_i)} > \eta\right) \varphi(\tau) d\tau \\
 &= \int_H^\infty \Pr\left(\frac{V_i g \xi^{NL}(\tau, f_i)}{I_\tau(f_i) + N(f_i)} > \eta\right) \varphi^{NL}(\tau) d\tau \\
 &\quad + \int_H^\infty \Pr\left(\frac{V_i g \xi^L(\tau, f_i)}{I_\tau(f_i) + N(f_i)} > \eta\right) \varphi^L(\tau) d\tau \\
 &= \int_H^\infty \Lambda^L \varphi^L(\tau) d\tau + \int_H^\infty \Lambda^{NL} \varphi^{NL}(\tau) d\tau.
 \end{aligned} \tag{30}$$

where  $\varphi^L(\tau)$  and  $\varphi^{NL}(\tau)$  are the PDF of RV  $\tau$ , when the UE is connected to a THz UAV BS having a LoS path and NLoS path, respectively.

According to [7], and considering that for UAV BSs the distance from the BS to the associated UE is equal to or larger than the UAV height, i.e.,  $\tau \geq H$ , we have (15) and (17).

Similarly, we can have (16) and (18). Moreover, based on [12], we have (19) and (20).

According to [7], we can also derive the the Laplace transform results expressed by (21), (22) and

$$\alpha = \frac{\xi^{NL}(v, f_i)}{\xi^L(v, f_i)}. \tag{31}$$

Substitute (2) and (3) and into (31), we have (23). ■

REFERENCES

- [1] C. Han and I. F. Akyildiz, "Three-Dimensional End-to-End Modeling and Analysis for Graphene-Enabled Terahertz Band Communications," *IEEE Trans. Veh. Technol.*, vol. 66, pp. 5626–5634, July 2017.
- [2] Z. Hossain, C. N. Mollica, J. F. Federici, and J. M. Jornet, "Stochastic Interference Modeling and Experimental Validation for Pulse-Based Terahertz Communication," *IEEE Trans. Wireless Commun.*, vol. 18, pp. 4103–4115, Aug. 2019.
- [3] T. Mao, Q. Wang, and Z. Wang, "Spatial Modulation for Terahertz Communication Systems With Hardware Impairments," *IEEE Trans. Veh. Technol.*, vol. 69, pp. 4553–4557, Apr. 2020.
- [4] X. Gao, L. Dai, Y. Zhang, T. Xie, X. Dai, and Z. Wang, "Fast Channel Tracking for Terahertz BeamSpace Massive MIMO Systems," *IEEE Trans. Veh. Technol.*, vol. 66, pp. 5689–5696, July 2017.
- [5] Y. Yang, M. Mandehgar, and D. R. Grischkowsky, "Understanding THz Pulse Propagation in the Atmosphere," *IEEE Trans. THz Sci. Technol.*, vol. 2, pp. 406–415, July 2012.
- [6] X.-W. Yao, C.-C. Wang, W.-L. Wang, and C. Han, "Stochastic geometry analysis of interference and coverage in Terahertz networks," *Nano Communication Networks*, vol. 13, pp. 9–19, Sept. 2017.
- [7] M. Ding, P. Wang, D. Lopez-Perez, G. Mao, and Z. Lin, "Performance Impact of LoS and NLoS Transmissions in Dense Cellular Networks," *IEEE Trans. Wireless Commun.*, vol. 15, pp. 2365–2380, Mar. 2016. arXiv: 1503.04251.
- [8] J. Kokkoniemi, J. Lehtomaki, and M. Juntti, "Stochastic Geometry Analysis for Mean Interference Power and Outage Probability in THz Networks," *IEEE Trans. Wireless Commun.*, vol. 16, pp. 3017–3028, May 2017.
- [9] J. Kokkoniemi, J. Lehtomaeki, and M. Juntti, "Stochastic Geometry Analysis for Band-Limited Terahertz Band Communications," in *2018 IEEE 87th Vehicular Technology Conference (VTC Spring)*, (Porto), pp. 1–5, IEEE, June 2018.

- [10] S. Zhang, H. Zhang, Q. He, K. Bian, and L. Song, "Joint Trajectory and Power Optimization for UAV Relay Networks," *IEEE Commun. Lett.*, vol. 22, pp. 161–164, Jan. 2018.
- [11] Y. Takahashi, Y. Kawamoto, H. Nishiyama, N. Kato, F. Ono, and R. Miura, "A Novel Radio Resource Optimization Method for Relay-Based Unmanned Aerial Vehicles," *IEEE Trans. Wireless Commun.*, vol. 17, pp. 7352–7363, Nov. 2018.
- [12] C. Liu, M. Ding, C. Ma, Q. Li, Z. Lin, and Y.-C. Liang, "Performance Analysis for Practical Unmanned Aerial Vehicle Networks with LoS/NLoS Transmissions," in *2018 IEEE International Conference on Communications Workshops (ICC Workshops)*, (Kansas City, MO), pp. 1–6, IEEE, May 2018.
- [13] J. R. Demers, F. Garet, and J.-L. Coutaz, "Atmospheric Water Vapor Absorption Recorded Ten Meters Above the Ground With a Drone Mounted Frequency Domain THz Spectrometer," *IEEE Sens. Lett.*, vol. 1, pp. 1–3, June 2017.
- [14] A. Saeed, O. Gurbuz, and M. A. Akkas, "Terahertz communications at various atmospheric altitudes," *Physical Communication*, vol. 41, p. 101113, Aug. 2020.
- [15] H. Elayan, O. Amin, R. M. Shubair, and M.-S. Alouini, "Terahertz communication: The opportunities of wireless technology beyond 5G," in *2018 International Conference on Advanced Communication Technologies and Networking (CommNet)*, (Marrakech), pp. 1–5, IEEE, Apr. 2018.
- [16] A. Moldovan, M. A. Ruder, I. F. Akyildiz, and W. H. Gerstacker, "LOS and NLOS channel modeling for terahertz wireless communication with scattered rays," in *2014 IEEE Globecom Workshops (GC Wkshps)*, (Austin, TX, USA), pp. 388–392, IEEE, Dec. 2014.
- [17] 3GPP, "Tr 36.828 (v11.0.0): Further Enhancements to LTE TDD for DL-UL Interference Management and Traffic Adaptation," 2016.
- [18] A.-A. A. Boulogeorgos and A. Alexiou, "Error Analysis of Mixed THz-RF Wireless Systems," *IEEE Commun. Lett.*, vol. 24, pp. 277–281, Feb. 2020.
- [19] B. Makki, C. Fang, T. Svensson, M. Nasiri-Kenari, and M. Zorzi, "Delay-Sensitive Area Spectral Efficiency: A Performance Metric for Delay-Constrained Green Networks," *IEEE Trans. Commun.*, vol. 65, pp. 2467–2480, June 2017.